Atlantic Electronic
Journal of Mathematics
Volume **2**, Number **1**, Summer **2007**

http://aejm.ca
http://aejm.ca/rema
pp. **30–54**

ON WEAKLY NONLINEAR DESCRIPTIONS OF NONLINEAR INTERNAL GRAVITY WAVES IN A ROTATING REFERENCE FRAME

Marek Stastna and Kristopher Rowe

Department of Applied Mathematics
University of Waterloo
200 University Avenue West
Waterloo, ON, N2L 3G1

Abstract. We discuss model equations for the description of horizontally propagating waves in the interior of a density stratified ocean in a rotating reference frame (e.g a rotating planet). Using linear theory we outline the complications the inclusion of rotation introduces. These complications preclude the strict application of equations in the classical Korteweg-de Vries (KdV) hierarchy. In place of the well-studied KdV-type equations, the so-called Ostrovsky equation is often employed to describe waves in the presence of rotation. However, this equation lacks the mathematical structure of the KdV equation, and in particular is not fully integrable. We present numerical integrations, based on spectral methods, of the Ostrovsky equation which show that solitary wave-like solutions decay slowly by radiating energy to a tail of dispersive waves. We discuss the shortcomings of the Ostrovsky equation and propose an alternative model equation that captures the linear, dispersive wave behaviour exactly.

1. **Introduction.** Experience tells us that most traveling waves do not retain their form as they propagate. For example, shoaling waves coming up onto the beach steepen and break. The wave steepening occurs due to the dependence of the wave propagation speed on the wave amplitude, and in particular, the fact that the taller parts of the waveform travel faster. A less dramatic, though equally universal, property of finite amplitude waves is the observation that waves with different wavelengths travel with different speeds. For example, throwing a rock into a still pond generates a disturbance with the shape of an expanding ring. Careful observation of the individual wave crests in the expanding ring reveals that these waves do not move with the same speed as the ring and hence disappear by either running out in front, or falling behind the ring. This phenomenon is referred to as dispersion.

The interior of large lakes and oceans is commonly observed to be density stratified, with lighter fluid found near the surface and heavier fluid found closer to the bottom. This density stratification provides a waveguide for a variety of waves. In nature, these waves are finite amplitude and hence exhibit wave steepening and wave dispersion. In this article we will consider the mathematical descriptions of internal waves that propagate horizontally, sometimes referred to as vertically trapped

2000 *Mathematics Subject Classification.* Primary: 35Q51, 76B15; Secondary: 76U05.
Key words and phrases. Solitons, gravity waves, rotating fluids.

waves. The surface manifestations of these waves are commonly observed from aircraft, satellites and the space shuttle and it is believed that such waves are important in the global budget of meridional heat transport by the oceans, in plankton and pollutant dynamics, as well as ocean acoustics, among other applications.

A full description of internal waves requires the consideration of an initial, boundary value problem for the Navier-Stokes equations with a moving boundary at the ocean's surface ([8]). Not only is a closed form solution of this problem not available, the very well-posedness of the problem has not been established. Indeed the solution of the well-posedness problem carries the million dollar Clay prize. From a more applied point of view, even the most powerful computers cannot handle the full range of space and time scales that must be resolved to successfully approximate the "real" ocean numerically. The situation, however, is not as hopeless as the preceding discussion makes it seem, as over a hundred years' worth of approximations, model equations and conceptual simplifications can be brought to bear on the problem, thereby providing us with a considerable level of understanding of internal waves in the ocean. In the following we will ignore the role of fluid viscosity and hence consider the Euler, as opposed to Navier-Stokes, equations. We will also make use of well-verified numerical solver for the Euler equations ([9]), and treat these numerical solutions as the gold standard by which to evaluate our simplified theories.

In this article we reconsider classical descriptions of weakly nonlinear long waves based on the Korteweg de Vries (henceforth KdV) equation. This equation allows for a balance between steepening due to nonlinearity and spreading due to dispersion, a balance that finds its expression in the existence of solitary wave solutions (nonlinear solutions which do not change form as they propagate). In fact, it is possible to analytically solve the Cauchy problem for the nonlinear KdV equation via a sequence of linear problems ([3]). The solution of the Cauchy problem reveals that, even though they are nonlinear, solitary wave solutions retain their identity during collisions. This particle-like behaviour has led to the term "soliton" in analogy with terms like "neutron" and "electron" in physics. The above described solution method, generally known as "the method of inverse scattering", stands as one of the truly great achievements of 20th century applied mathematics and has spawned a vast and diverse literature (see [1] for a relatively recent monograph).

The application of the KdV equation to internal waves dates back to Benney, who in 1966 employed an asymptotic expansion in amplitude and aspect ratio (the ratio between wavelength to water depth) to reduce the equations of fluid mechanics to a Sturm Liouville problem for the vertical structure and the KdV equation for the horiozntal and temporal structure ([2]). Benney's approach has been extended to account for a wider variety of physical phenomena ([5]). While the literature is voluminous, it is fair to say that KdV type theories (often referred to as model equations) have provided an important qualitative method in understanding the life cycle of internal waves, from their generation, through propagation through to dissipation and breakdown. However quantitative comparisons with experimental data, observations and numerical simulations have unambiguously revealed that the KdV equation cannot account for the precise shape and propagation speed of finite amplitude waves.

In this article, we focus on the description of internal waves in a rotating frame of reference. Including the effects of rotation precludes exact solitary wave solutions, modifies the form of the governing equation (often called the Ostrovsky equation,

[4]), and presents problems when constructing numerical approximation schemes ([7]). We present a phenomenological governing equation that improves the representation of wave dispersion in a rotating frame of reference, construct a spectral discretization scheme based on the Fast Fourier Transform (FFT), and discuss numerical integrations for both standard soliton fissioning problems and comparisons with integrations of the full Euler equations.

2. **Background Material.** The results we discuss deal with approximate descriptions of fluid motions. While the details of how these approximations are derived are beyond this article, we will begin with a qualitative description of the approximation process in order to provide the reader with a broad perspective on the material that follows.

The mathematical description of the motion of a fluid is given a system of nonlinear partial differential equations that express the conservation laws of classical physics (the conservation of mass, linear momentum and energy) as they apply to a flowing continuum. When the viscosity (stickiness) of a fluid is neglected, as is commonly done in the description of motions in the atmosphere and the ocean, the so–called Euler equations for an incompressible, rotating fluid are first–order and read

$$\rho_0[\frac{\partial \vec{u}}{\partial t} + \vec{u}\cdot\vec{\nabla}\vec{u} + 2\vec{\Omega}\times\vec{u}] = -\vec{\nabla}p - \rho g\hat{k} \quad (1)$$

$$\vec{\nabla}\cdot\vec{u} = 0 \quad (2)$$

$$\frac{\partial \rho}{\partial t} + \vec{u}\cdot\vec{\nabla}\rho = 0. \quad (3)$$

Here $\vec{u}$ is the fluid velocity, ρ the density, ρ_0 the constant 'reference' density, p the fluid pressure, $\vec{\Omega}$ the constant rotation vector of the Earth, and $\hat{k}$ the unit vector in the vertical direction. Note that we have made the so–called Boussinesq approximation which neglects density changes except in the buoyancy term $\rho g\hat{k}$, though this detail is unimportant for the development below. The Euler equations suffer from two mathematical difficulties. The first is the presence of quadratic nonlinearities associated with the $\vec{u}\cdot\vec{\nabla}$ portion of the equations. The second is the lack of an evolution equation for pressure (though the system is formally closed since we have five equations for the five unknowns).

It is often observed that the density has a vertically varying profile that is largely independent of time with small amplitude perturbations superimposed upon this basic state, so that

$$\rho = \rho_0(\bar{\rho}(z) + \rho').$$

Such fluids are referred to as *stratified*, and for static stability (i.e. if we set $\vec{u} = \vec{0}$) we require that density decreases in the vertical direction, or that $d\bar{\rho}/dz < 0$ (we are implicitly assuming that $\bar{\rho}(z)$ is differentiable). The stratification in the fluid serves as a wave guide, and a parameter employed in the description of such waves is proportional to the rate of change of density with height and is often called the buoyancy or Brunt–Vaisala frequency squared, and written as

$$N^2(z) = -g\frac{1}{\rho_0}\frac{d\bar{\rho}(z)}{dz}.$$

While stratified fluids can exhibit waves that propagate in any direction we will only consider so–called vertically trapped waves that propagate horizontally. If we now consider two dimensional flow, for example if we align the x–axis with the direction

of wave propagation, ignore changes in the across–wave direction and take the z axis to point upward, then the divergence–free condition $\vec{\nabla} \cdot \vec{u} = 0$ guarantees the existence of a stream function ψ so that $\vec{u} = (u, w) = (\psi_z, -\psi_x)$, where subscripts denote partial derivatives. The Euler equations can then be reduced to an evolution equation for the streamfunction ψ and the so–called buoyancy $b = -g\rho'$. The reduction involves a curl of the momentum equations (1) and thus eliminates the pressure variable from consideration.

Approximate theories next assume a separation of variables in which

$$\psi(x, z, t) = A(x, t)\phi(z)$$

and seek an ordinary differential eigenvalue problem for the so–called vertical structure function $\phi(z)$ and a partial differential equation for the horizontal structure function $A(x, t)$. A particularly simple case is obtained if we concentrate on long waves, or waves in the limit of small wave number, $k \to 0$. Linear theory assumes the nonlinear terms can be dropped and, after some algebra, one finds that in this case $A(x, t)$ satisfies the linear wave equation $A_{tt} = c^2 A_{xx}$ where c is determined from the eigenvalue problem for the vertical structure function (details are discussed in the following section).

Linearization formally assumes that waves are of infinitesimal amplitude. Actual waves, of course, have a finite amplitude, and finite amplitude waves are observed to be modified in two ways. First, the waves can steepen due to the amplitude dependence of the propagation speed. Second, waves of different wavelengths propagate with different speeds, or the waves are dispersive. While nonlinear steepening cannot be represented in linear theories, dispersion can (a rather odd property of classical field theories like fluid mechanics and electricity and magnetism). However the governing equation, while still a sort of linear wave equation, is no longer hyperbolic. Indeed, the vast majority of waves observed in the physical world are not the tidy hyperbolic waves studied in virtually every introductory course on partial differential equations.

Internal wave theories, following Benney's pioneering 1966 article, generally begin with linear long-waves (the wave number, k is taken to tend to zero, as mentioned above) and seek corrections to the linear wave equation for $A(x, t)$ which is generally assumed to be uni-directional (most often for rightward propagating waves). This is done via an asymptotic expansion of $\psi(x, z, t)$ in two small parameters, one measuring the wave amplitude (often called the nonlinearity parameter and labeled ϵ) and a different parameter measuring the mismatch between the long horizontal and short vertical scales (often called the dispersion parameter and labeled μ). The expansion yields,

$$\psi(x, z, t) = A(x, t)\phi(z) + \epsilon\psi^{(1,0)} + \mu\psi^{(0,1)} + ...$$

and when both first order corrections are considered, the well known Korteweg de Vries equation for $A(x, t)$, discussed in detail below, results.

Benney's article did not consider rotation (the $2\vec{\Omega} \times \vec{u}$ term in the Euler equations was dropped) and in this case the linear long-waves propagate faster than any other linear waves. As we will show below, rotation invalidates this finding, as far as the propagation of energy is concerned. Thus in the rotation–modified case the asymptotic procedure must be modified. This is done by the introduction of a third small parameter measuring the strength of rotation effects (Benney's assumption amounts to a restriction on time scales less than 12 hours or so on Earth). The

resulting asymptotic expansion requires a great deal more algebra, but we should be clear at the outset that it cannot truly make up for the fact that the long waves no longer travel faster than other linear waves. It is one of the purposes of this article to show that the weakly nonlinear description of internal waves modified by rotation can be improved by considering the complete linear dispersion relation *a posteiori* for the linear part of the weakly nonlinear equations derived by asymptotic theories.

3. **Dispersion and Linear Theory.** Before we consider weakly nonlinear, or KdV-type, theories, it is worthwhile to reconsider purely linear theories. In the original Benney 1966 formulation, linear internal waves have a vertical structure governed by the following Sturm Liouville eigenvalue problem (subscripts denote partial derivatives)

$$\begin{aligned} \phi_{zz} + \left(\frac{N^2(z)}{c(k)^2} - k^2 \right) \phi &= 0 \\ \phi(0) = \phi(H) &= 0. \end{aligned} \tag{4}$$

Here H is the total water depth, z is the vertical coordinate (so that $z = 0$ is the ocean bottom and $z = H$ is the ocean surface, under the so–called rigid lid approximation [8]), k is the wave number, $c(k)$ is the speed with which individual crests move (or phase speed equal to the frequency divided by the wave number), and $N^2(z)$ is the square of the so-called buoyancy frequency ([8]) and depends on the variation of density with depth at a particular location. A widely applicable, though by no means unique, form of $N^2(z)$ is

$$N^2(z) = N_0^2 \text{sech}^2(\frac{z - z_0}{d}) \tag{5}$$

which corresponds to a rapid change in density near $z = z_0$ and little change outside of this so-called "pycnocline" region. When d is small, this stratification is an excellent approximation for experimental realizations in which a layer of light fluid overlies a layer of heavy fluid with molecular diffusion smearing out the interface. Analytical studies generally adopt the more restrictive assumption of constant $N^2(z) = N_0^2$. In this latter case the eigenfunctions are given by

$$\phi(z) = \sin\left(\frac{n\pi z}{H}\right) \tag{6}$$

for any $n = 1, 2, 3, ...$ with corresponding phase speeds (the speed with which wave crests move)

$$c(k) = \frac{N_0 H}{\sqrt{n^2\pi^2 + (kH)^2}}. \tag{7}$$

It is clear from (7) that longer waves ($k \to 0$) travel faster and that waves with larger n travel more slowly. From (6) we can see that the eigenfunction has $n - 1$ zeroes in the interior of the fluid. Considering only the longwave limit, $k = 0$ it is further possible to show that the largest eigenvalue corresponds to waves for which the lines of constant density are displaced either upwards or downwards at all points in the interior of the domain. Such waves are called mode-1 waves in the internal wave literature and are the only waves we will discuss for the remainder of this article. While the present results formally hold for any mode, it is generally observed that a vast majority of the energy in the internal wave field (in a lake or coastal ocean) is found in the first mode. The description of higher modes also requires consideration of interactions between modes, which, while interesting, is far too large of a topic

to be tackled in this article. Note that, using classical Sturm Liouville theory, it is possible to show that the above results are general for arbitrary $N^2(z)$ as long as $N^2(z) \geq 0$ at all z ([12]).

Once the phase speed is found as a function of k, linear theory consists of writing an initial condition as a "sum" of Fourier components, either via Fourier Transforms or Fourier series. Subsequently the evolution of each Fourier constituent is carried out independently and the solution at some later time t can be reconstructed either by summation, or the inverse Fourier transform. The former is easy, though inefficient, to implement numerically and yields

$$A(x,t) = \frac{a_0}{2} + \sum_{n=1}^{N} a_n \exp\left(ik_n[x - c(k_n)t]\right)$$

where the initial condition has the Fourier expansion

$$A(x,0) = \frac{a_0}{2} + \sum_{n=1}^{N} a_n \exp\left(ik_n x\right).$$

More efficient numerical algorithms are no more complicated conceptually, but employ the the Fast Fourier Transform algorithm (or FFT) to carry out the Fourier reconstruction efficiently. Such method are referred to as spectral methods (though not all references to spectral methods involve the FFT, [11])).

For internal waves in a rotating frame of reference the eigenvalue problem is somewhat different in that instead of solving for the phase speed, the frequency is determined from the eigenvalue problem

$$\begin{aligned} f^2\phi_{zz} - k^2N^2(z)\phi \quad &= \quad \omega(k)^2[\phi_{zz} - k^2\phi] \\ \phi(0) = \quad \phi(H) \quad &= 0. \end{aligned} \tag{8}$$

It is useful to rewrite the above using linear differential operators as

$$\mathcal{A}\phi = \lambda\mathcal{B}\phi$$

where $\lambda = \omega^2$,

$$\mathcal{A}\phi = f^2\phi_{zz} - k^2N^2(z)\phi$$

and

$$\mathcal{B}\phi = \phi_{zz} - k^2\phi.$$

In practice, ϕ is conisdered at a finite number of grid points and the derivatives are replaced by either a finite difference or pseudo-spectral approximation, thereby yielding a generalized eigenvalue problem for matrices

$$A\phi = \lambda B\phi$$

amenable to standard solution algorithms (using Matlab or its freeware counterpart, Octave, for example). On Earth, the magnitude of the Coriolis parameter $|f|$ ranges from 0 at the equator to $\pm 1.46 \times 10^{-4}$ s^{-1} at the poles (positive in the north). Of course, rotating tables in the laboratory can have much larger values of f. In the simulations we discuss we have chosen three different values of f that yield qualitatively different behaviour. All are too high compared to values measured on Earth. The results should thus be interpreted as being qualitative, as opposed to a model of any particular geographic location.

Again, it is useful to consider $N^2(z) = N_0^2$ as a simple (if somewhat unrealistic) case in which (8) has an analytical solution. Direct substitution confirms that the mode-1 solution is again given by the eigenfunction

$$\phi(z) = \sin\left(\frac{\pi z}{H}\right)$$

and the dispersion relation

$$\omega(k)^2 = \frac{f^2 + k^2 \frac{H^2 N_0^2}{\pi^2}}{1 + k^2 \frac{H^2}{\pi^2}}. \tag{9}$$

From (9) we can see that for long waves ($k \to 0$) the frequency tends to f while for short waves ($k \to \infty$) the frequency tends to N_0. The fact that the frequency is bounded in the longwave limit implies that the phase speed grows without bound as $k \to 0$. For a given parameter set it is possible to show that the group speed

$$c_g(k) = \frac{d\omega(k)}{dk}$$

is bounded for all k and has a single maximum. This is in stark contrast to the non-rotating case for which the long waves have the largest value of both phase and group speed. Thus, if we create an initial disturbance in a nonrotating frame of reference and measure the waves that arrive at a measuring site some distance away, the long waves will arrive first. In a rotating frame of reference the length of the waves that arrive first has to be determined on a case by case basis.

As mentioned above, the most common experimentally realized density stratification is that of a layer of light fluid overlying a layer of heavier fluid, separated by a thin interface. For the remainder of this article we consider this stratification in water 100 m deep with $N_0 = 0.14$ s^{-1}, $z_0 = 20$m and $d = 5$ m. By solving the eigenvalue problem (8) we find frequency, phase speed and group speed given by the curves in figure 1 for various values of f. It is clear that they are in qualitative agreement with the discussion above for the constant N^2 case.

In figure 2 we present a solution of the linear problem based on the dispersion relations shown in figure 1 using 5000 terms in the Fourier series. We consider output from a well-resolved numerical simulation of the Euler equations as an initial condition, find a Fourier decomposition of the initial condition, advance each component forward in time according to the dispersion relation, and finally rebuild the waveform at the later time (14,000 s, or 3.9 hours is used for the figure). Panels 2a and 2b show the initial conditions used for the simulations shown in panels 2c and 2d, respectively. Panels 2c and 2d show the output from both the fully nonlinear simulation (dashed line) and the linear model (solid line). It is clear that when rotation is weak (and indeed for all values of f relevant to the Earth) the linear model fails to successfully predict the evolution of the wave disturbance. In particular, the errors are largest in the leading, large amplitude structure, thereby suggesting that nonlinearity is importnat. For stronger rotation, shown in figure 2b, the linear theory is extremely good for the leading wave packet with some errors in the phase of the waves found in the trailing tail. The linear theory does break down for times longer than those shown ($t \gg 4$ hours) even for the higher rotation case.

4. **Weakly Nonlinear Theory.**

4.1. **KdV Model.** The above results demonstrate that our simple linear model is not sufficient to represent the behavior of internal gravity waves in cases of low to moderate rotation. We thus turn our attention to weakly nonlinear models. We begin with the well studied KdV equation for rightward propagating longwaves (subscripts denote partial derivatives with respect to x and t),

$$A_t = -c_{lw}A_x + 2r_{10}c_{lw}AA_x + r_{01}A_{xxx} \tag{10}$$

where c_{lw},r_{10}, and r_{01} are physical parameters, measuring the linear long wave speed, the strength of nonlinearity and the strength of dispersion, respectively. The two parameters r_{10} and r_{01} are derived from the first order corrections to the vertical structure equation by invoking the Fredholm Alternative. Detailed discussions can be found in the literature ([2] and [10]). For a given stratification all three parameters are determined uniquely from the eigenvalue problem (4) with $k = 0$ ([10]), or in other words from

$$\begin{aligned} \phi_{zz} + \frac{N^2(z)}{c_{lw}^2}\phi &= 0 \\ \phi(0) = \phi(H) &= 0. \end{aligned} \tag{11}$$

For rightward propagating waves $c_{lw} > 0$ and it is a simple matter to show that $r_{01} < 0$ while r_{10} may be of either sign. This means we could redefine $r_{01}^* = -r_{01}$ and have r_{01}^* be strictly positive. We do not do so, following the general approach adopted in the internal wave literature. The theory of the KdV equation, as discussed in standard texts is presented in what is known as standard form ([3])

$$B_t - 6BB_x + B_{xxx} = 0.$$

This form can be obtained from (10) by simple coordinate transformations. For the present discussion the physical form is more appropriate. Making use of the Fourier transform

$$\mathcal{F}[A(x,t)] = \int_{-\infty}^{\infty} \exp(-ikx)A(x,t)dx$$

so that

$$\mathcal{F}[A_x] = ik\mathcal{F}[A]$$

the KdV equation may be rewritten in Fourier space as

$$\bar{A}_t = -ik(c_{lw} + r_{01}k^2)\bar{A} + r_{10}c_{lw}\bar{A}^2 \tag{12}$$

where the overbar denotes a Fourier transformed function and in the final term the transform is taken after squaring A. Notice that if the nonlinear term is ignored (12) tells us that the model of the phase speed as a function of wave number that is employed in the KdV equation is

$$c_p(k) = c_{lw} + r_{01}k^2 \tag{13}$$

and hence (since $r_{01} < 0$) that shorter waves travel slower. While this is a desirable property, notice that when

$$k > \sqrt{\frac{c_{lw}}{|r_{01}|}} \tag{14}$$

we have $c_p(k) < 0$ and hence the KdV equation makes the contradictory prediction that short waves assumed to be rightward propagating, in fact travel to the left. This shortcoming of the KdV theory is due to the fact that the theory is a long wave theory, and hence only formally valid as $k \to 0$.

The spectral form (12) is of great advantage in designing and implementing numerical methods for the KdV equation. All that is required is a stable time-stepping method and a way to carry out the Fourier transform ([11]). In practice the FFT will be used. In the case of an explicit Euler scheme the time–stepping proceeds in the following way: we compute $A(x,t)^2$, take its Fourier transform, take the Fourier transform of $A(x,t)$, step forward in Fourier space according to (12), and finally inverse Fourier transform back to physical space. For all the simulations reported below the somewhat more complicated, though equally standard, fourth-order Adams-Bashfroth scheme ([6]) has been implemented. A difficulty that arises in applying this algorithm is the relative numerical sensitivity of the KdV equation. To avoid using an impractically small time-step to maintain numerical stability, one can apply an integrating factor

$$I = e^{-(c_{lw} ik + r_{01} ik^3)t}$$

to the equation obtained after taking the Fourier Transform. The resulting equation can then be solved in terms of a new variable $\tilde{A} = I\bar{A}$ with the dispersive terms now solved for exactly ([11]).

In figure 3 we show an example of an initial Gaussian perturbation fissioning into a rank-ordered train of solitary waves (or solitons). As can be confirmed by standard KdV theory, the largest amplitude solitary waves are thinnest and travel fastest. For longer times the wave train would continue to spread out, with the tallest waves running farther and farther ahead of the shorter waves.

4.2. **Models with Rotation.** The KdV model takes us a step in the right direction by introducing a nonlinear term, thereby allowing for a balance between dispersion and nonlinearity that makes solitary waves possible. While this is a considerable improvement over linear theory, for internal waves in a rotating frame of reference the dispersion behaviour contained in the KdV equation is qualitatively incorrect. A successful model equation needs to reflect the fact that frequency remains bounded for long waves, and hence that the phase speed grows without bound as $k \to 0$. Such a theory has been formally derived by several authors, again via an asymptotic expansion, but now in three small parameters. In the literature the resulting equation is generally referred to as the Ostrovsky equation ([4]), and employing the same notation as for the KdV equation reads

$$A_{xt} = -c_{lw} A_{xx} + 2r_{10} c_{lw} (AA_x)_x + r_{01} A_{xxxx} + \gamma A, \tag{15}$$

where γ is a constant measuring the strength of rotation effects.

It is a simple matter to confirm that when the nonlinear term is neglected, the Ostrovsky equation yields the dispersion relation

$$\omega(k) = c_{lw} k + r_{01} k^3 + \gamma \frac{1}{k} \tag{16}$$

so that not only do we have that the phase velocity grows without bound for long waves, but that $\omega(k)$ does as well. The latter is in stark contrast to the correct limiting behaviour: $\omega \to f$ as $k \to 0$. In figure 4a and 4b we show the phase and group velocity, respectively, as a function of k for the linearized KdV, linearized Ostrovsky and true linear cases. For all three models we employ the single pycnocline stratification (5), and we set $f = 0.00071$. It is clear that while both the KdV and Ostrovsky equations predict incorrect dispersion behaviour for both long and short waves, all three models are in good agreement for the middle third of the domain shown. This range corresponds to waves with length scales between 700 and

1600 m. Furthermore, figure 4 shows that the Ostrovsky model gives qualitatively correct behaviour in the long wave limit.

The asymptotic theory that yields the Ostrovsky equation provides a certain amount of freedom in the exact value of γ (it is related to the typical length scale in the direction transverse to the direction of propagation, something that is reasonably clear in an experimental tank, but not the coastal ocean), unlike the other coefficients which are fixed precisely by the physical situation. For the present simulations γ was selected so as to yield the best overall match between the solutions of the Ostrovsky equation and numerical integrations of the full Euler equations. These simulations will be discussed in detail below.

In figure 5 we repeat figure 4 for a larger rotation rate. It is clear that the while the Ostrovsky equation yields an approximation of the correct dispersion behaviour with roughly the same qualitative behaviour as in the lower rotation case, the match of the three theories for waves with intermediate length scales is not nearly as good as in the lower rotation case.

The Ostrovsky equation, while qualitatively similar to the KdV in appearance, does not share the mathematical structure of the KdV that allows the latter to be solved semi-analytically. This means that while we do expect solitary-like waves that decay only very slowly, we do not expect true solitary waves for the Ostrovsky equation. The smaller the value of the rotation parameter γ, the closer the evolution should be to that predicted by the KdV theory.

The Ostrovsky equation is solved by a FFT-based spectral method with fourth order Adams-Bashforth time stepping. As is commonly done in the literature ([7]), we first integrate to get

$$A_t = -c_{lw}A_x + 2r_{10}c_{lw}AA_x + r_{01}A_{xxx} + \gamma\int_x^\infty A(s,t)ds$$

and then discretize a Fourier-transformed version of this equation in time using an Adams-Bashforth method. Care must be taken near the end-points of the finite integration domain to ensure that spurious oscillations that develop there do not propagate into the interior of the computational domain and corrupt the phenomena of interest.

In figure 6 we initialize the Ostrovsky equation with an exact KdV solitary wave. In figure 6a $\gamma = 6.1 \times 10^{-8}$ (corresponding to the case $f = 0.00071$ s^{-1}) and we see that after 1.5 hours the solitary-like wave has propagated nearly 12 kilometers with the only visible change being the development of a very broad, small amplitude tail. In contrast, for the higher rotation rate of $f = 0.003$ s^{-1} ($\gamma = 1.83 \times 10^{-6}$) the leading solitary wave decays considerably, while a trailing solitary-like wave grows in amplitude. The leading solitary-like wave will slowly decay while the trailing wave grows. The trailing wave will gradually overtake the disappearing leading wave. At this point in time another trailing wave will begin to form and the process is repeated. This process is visible in figure 7 in which we show the wave profiles as a surface plot with the space variable running along the page and the time variable running into the page. The two overtaking waves are trailed by a tail of long dispersive waves with a wavelength of roughly 4 kilometers.

In figure 8 we reconsider the case of the simulation shown in figure 2c for which linear theory failed to accurately approximate the fully nonlinear simulation results. The initial condition is shown in panel 8a and the solution of the Ostrovsky model 1400s later is compared to the fully nonlinear simulation in panels 8b and 8c. Panel 8c shows the dispersive wave tail in detail for the same time as panel (b). It

is clear that while the Ostrovsky equation is reasonably accurate in predicting the amplitude of the leading overtaking solitary-like waves and the various waves that make up dispersive wave tail, the Ostrovsky model makes an error in the phase of both the leading overtaking solitary-like waves and the dispersive wave tail. Nevertheless, in contrast to the linear model the qualitative aspects of the evolution are well represented.

When the rotation is further reduced to $f = 0.00071$ s^{-1} the leading wave is essentially a slowly decaying solitary wave. In figure 9 the predictions of the Ostrovsky model are shown in the same manner as figure 8. From panel 9b we can see that the main error is in the propagation speed of the leading solitary-like wave. Furthermore, from panel 9c we can see that the description of the dispersive wave tail again exhibits a small phase error.

5. **Fully Dispersive Model.** While the predictions of the Ostrovsky model discussed in the previous subsection were reasonably accurate, as far as they successfully model the damping by wave radiation of an initial solitary wave, two issues remain outstanding. The first is the choice of the constant γ and the second is the singularity of the frequency $\omega(k)$ at $k = 0$. Both issues can be addressed by considering a model that employs the exact linear dispersion relation (referred to as the "fully dispersive model" in the following and "F D model" in the figure legends). Note that this does not mean that we incorporate all dispersion into this model, since in the asymptotic expansion discussed in section 2 beginning with terms of order $\epsilon\mu$ we would find terms that are both nonlinear and dispersive. Nor is this modification rigorously derived. Nevertheless, we will find it to yield greatly improved results when compared with the Ostrovsky equation.

In Fourier space we write

$$\bar{A}_t = -c_{lin}(k)ik\bar{A} + r_{10}c_{lw}ik\bar{A}^2 \tag{17}$$

where $c_{lin}(k)$ is the phase speed obtained by solving the eigenvalue problem (8) for various k. This means we consider the dispersive behaviour to be exactly given by the linear theory with nonlinearity represented by a quadratically nonlinear correction term. In practice the numerical code for the solution of (17) can contain a solver for (8) or the dispersion relation can be fitted using standard curve-fitting techniques, and the resulting analytical expression for $c_{lin}(k)$ used in (17).

In figure 10 we reconsider the evolution of a KdV solitary wave for $f = 0.0071$ (panel 10a) and $f = 0.003$ (panel 10b). It can be seen that the low rotation case leads to a slow decay, mainly due to the generation of a long trailing shelf. By comparing with figure 6a it can be seen that the fully dispersive model predicts a longer, and slightly larger shelf than the Ostrovsky model. The evolution of the higher rotation case, shown in panel 10b, has a similar qualitative character to figure 10b, but the decay of the leading wave is slower than in the Ostrovsky model.

In figures 11 and 12 we compare the predictions of the fully dispersive model with the fully nonlinear simulations. It can be seen that the leading wave still propagates slower than in the fully nonlinear simulations. However, the errors in the dispersive tail are significantly reduced. Indeed, it is fair to conclude that the fully dispersive model, which is transparent in its (albeit phenomenological) derivation, performs better than the more complicated Ostrovsky theory.

6. **Conclusions.** We have considered several reduced models for describing the propagation of internal gravity waves on a rotating planet. The primary effect of

rotation is to preclude the existence of exact solitary wave solutions, and hence preclude the application of completely integrable equations like the KdV equation. Indeed when the rotation is strong enough linear theory does a rather good job of describing the wave propagation, since the majority of the energy in an initial disturbance does not propagate and any resulting waves are extremely small in amplitude. For rotation rates typical of Earth, however, linear theory fails almost entirely. The wave dynamics involves slowly decaying (often called radiation-damped) solitary-like waves trailed by sizable, and complex tails of dispersive waves.

We have demonstrated that the most commonly discussed weakly nonlinear asymptotic theory (based on the KdV equation, which balances nonlinearity and dispersion), that of the so–called Ostrovsky equation, gives qualitatively reasonable results for the wave dynamics, but is plagued by a singularity of the frequency in the long wave limit. This singularity finds its expression in the amplitude and phase of the dispersive wave tail, and more importantly, leads to difficulties in constructing numerical approximations. In contrast, we have argued that a phenomenological weakly nonlinear evolution equation that incorporates the dispersion properties of linear waves exactly (to the limit of numerical precision) provides results superior to the Ostrovsky equation both in terms of numerical stability and wave dynamics.

The results of this article complement those in ([10]) for modeling undular bores without rotation using various weakly nonlinear theories (including one theory in which the full linear dispersion is used). It may be possible to extend the phenomenological evolution equation proposed above to include nonlinear terms that more accurately model the variation of solitary wave propagation speeds with wave amplitude. Future work could also consider the wave generation process, comparing a forced 'exact' equation to the more classical forced KdV equation. This is a promising direction since the fully dispersive theory could allow for a more completely exploration of phase space with the full Euler equations subsequently used to examine particularly noteworthy phenomena.

Acknowledgements. The authors would like to acknowledge the support of the University of Waterloo Work Placement program (K.R.) and NSERC (M.S.). The comments of an anonymous reviewer greatly improved both the content and presentation of this article.

REFERENCES

[1] M.J. Ablowitz, P.A. Clarkson, Solitons, Nonlinear Evolution Equations and Inverse Scattering, London Mathematical Society Lecture Notes 149, Cambridge University Press, Cambridge, 1991.

[2] D.J. Benney, *Long nonlinear waves in fluid flows*, Journal of Mathematics and Physics, textbf45, 1966, 52–78.

[3] P. G. Drazin, R.S. Johnson, Solitons: an Introduction, Cambridge University Press, Cambridge, 1989.

[4] R. Grimshaw, *Evolution Equations for Weakly Nonlinear Internal Waves in a Rotating Fluid*, Studies in Applied Mathematics, **73**, 1985, 1–33.

[5] R. Grimshaw, *Internal Solitary Waves* in Advances in Coastal and Ocean Engineering, ed. P., L-F. Liu, World Scientific Publishing, Singapore, 1997.

[6] A. Iserles, A First Course in the Numerical Analysis of Differential Equations, Cambridge University Press, Cambridge, 1996.

[7] C. Katsis, T.R. Akylas, *Solitary internal waves in rotating channels: A numerical study*, Physics of Fluids, **30** no. 2, 1987, 297–301.

[8] P. Kundu, I.M. Cohen, Fluid Mechanics, 3rd ed., Elsevier Academic Press, San Diego, 2004.

[9] K.G. Lamb, *Numerical experiments of internal wave generation by strong tidal flow across a finite amplitude bank edge*, Journal of Geophysical Research, **99** no. C1, 1994, 843-864.
[10] K.G. Lamb, L. Yan, *The evolution of internal wave undular bores: Comparisons of a fully nonlinear numerical model with weakly nonlinear theory*, Journal of Physical Oceanography, **26**, (1996), 2712–2734.
[11] L.N. Trefethen, Spectral Methods in Matlab, SIAM, Philadelphia, 2000.
[12] C. Yih, Dynamics of Nonhomogeneous Fluids, Macmillan, New York, 1965.

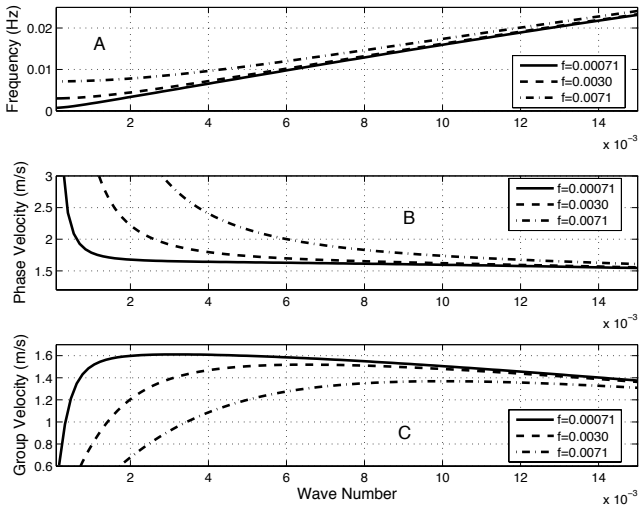

FIGURE 1. The frequency (A), phase speed (B), and group speed (C), as functions of wave-number according to the linear theory of internal gravity waves on a rotating planet. Note in particular that the group speed has a well defined maximum for $k > 0$.

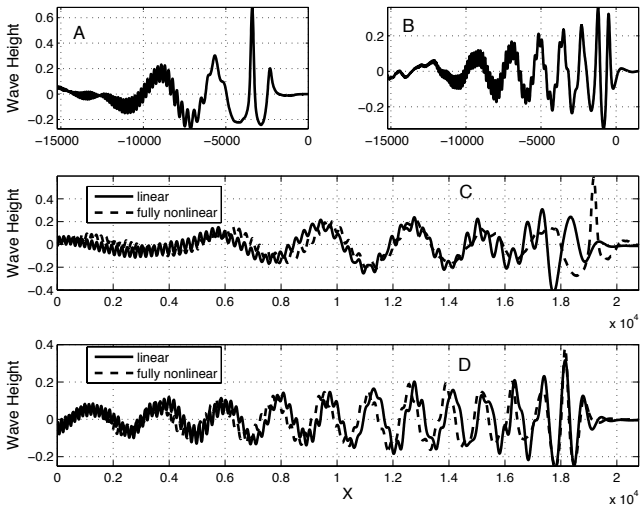

FIGURE 2. The evolution of two initial states taken from a simulation of the full Euler equations, (A) medium rotation, (B) high rotation. For the final states 3.9 hours later ((C) medium rotation, (D) high rotation) the predictions of linear theory are shown as solid lines, the 'exact' solution is indicated by a dashed line.

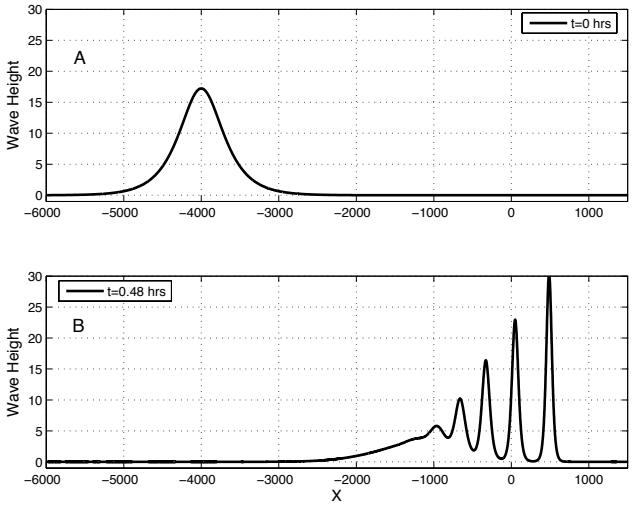

FIGURE 3. The evolution of an initial Gaussian state (A) for the KdV equation, showing the fissioning of a rank-ordered train of solitons (B).

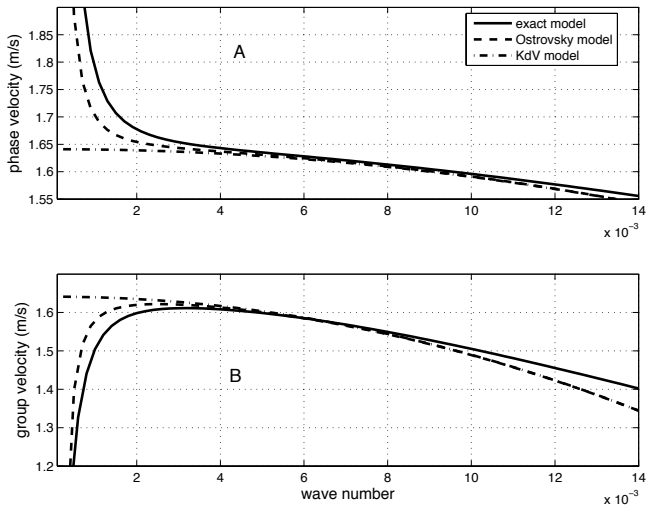

FIGURE 4. A comparison of the dispersion behaviour of the exact linear (solid), linearized Ostrovsky (dashed) and linearized KdV (dot-dashed). Phase and group velocities are shown in panels (A), and (B), respectively. $f = 0.00071\ \mathrm{s}^{-1}$, or low rotation case.

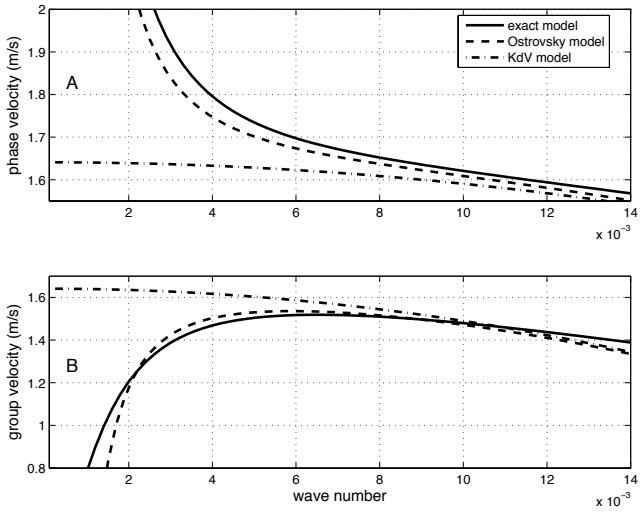

FIGURE 5. A comparison of the dispersion behaviour of the exact linear (solid), linearized Ostrovsky (dashed) and linearized KdV (dot-dashed). Phase and group velocities are shown in panels (A), and (B), respectively. $f = 0.0030$ s^{-1} or medium rotation case.

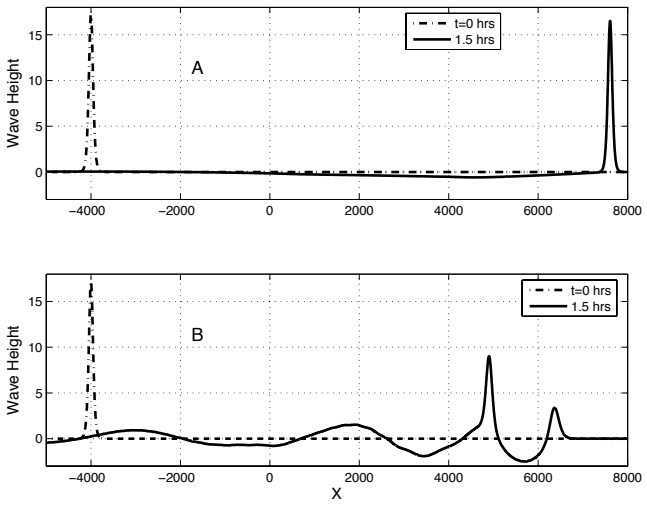

FIGURE 6. The evolution and radiative decay of a KdV solitary wave for the Ostrovsky model after 1.5 hours. Panels (A) and (B) show the cases of low ($f = 0.00071$ s^{-1}) and medium ($f = 0.0030$ s^{-1}) rotation, respectively.

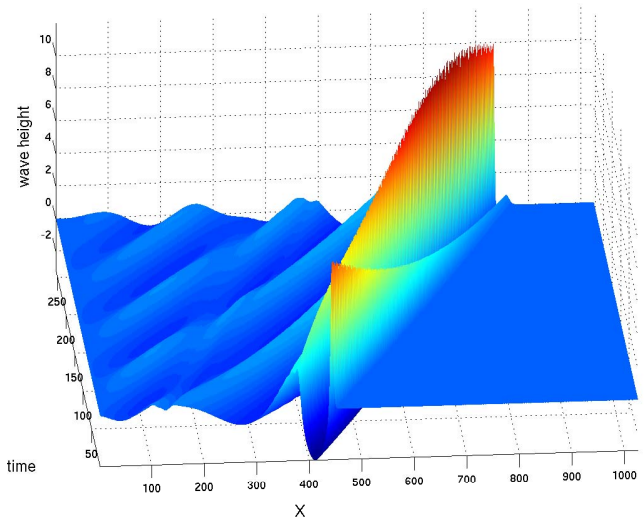

FIGURE 7. A surface plot showing the decay of the leading solitary-like wave due to rotation for the Ostrovsky model. Note the growth of a secondary wave that will eventually overtake the first. Space runs along the page and time runs into the page. $f = 0.0030$ s^{-1} or medium rotation.

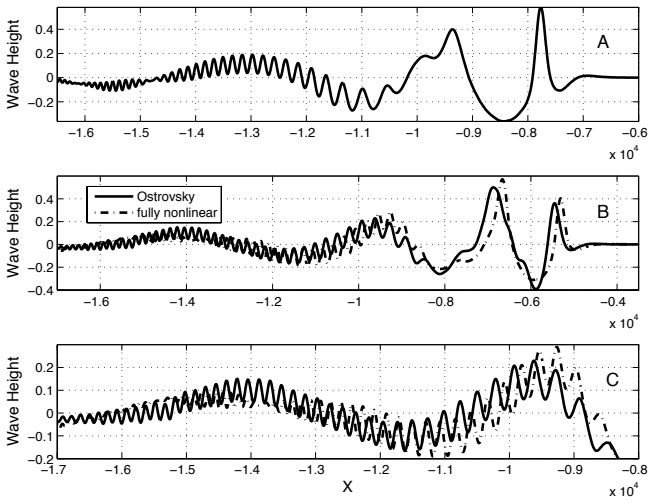

FIGURE 8. The evolution of an initial disturbance (panel (A)) taken from a simulation of the full Euler equations. Panel (B) shows the prediction of the Ostrovsky equation (solid) and the fully nonlinear simulation (dot-dashed) after $1,400$ seconds. Panel (C) shows the detail of the dispersive wave-tail. $f = 0.0030$ s^{-1} or medium rotation.

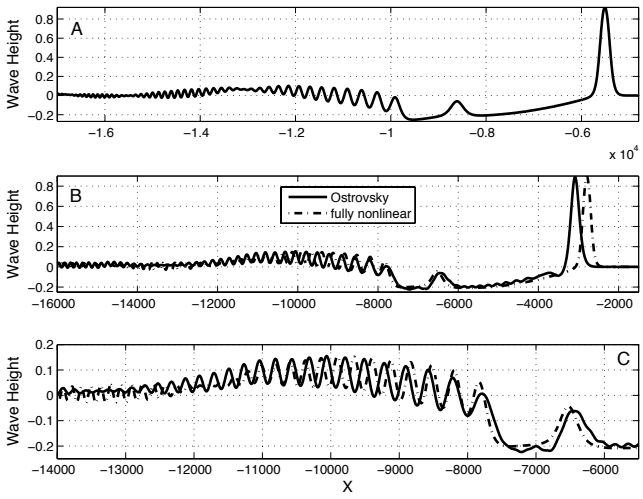

FIGURE 9. The evolution of an initial disturbance (panel (A)) taken from a simulation of the full Euler equations. Panel (B) shows the prediction of the Ostrovsky equation (solid) and the fully nonlinear simulation (dot-dashed) after $1,400$ seconds. Panel (C) shows the detail of the dispersive wave-tail. $f = 0.00071$ s^{-1} or low rotation.

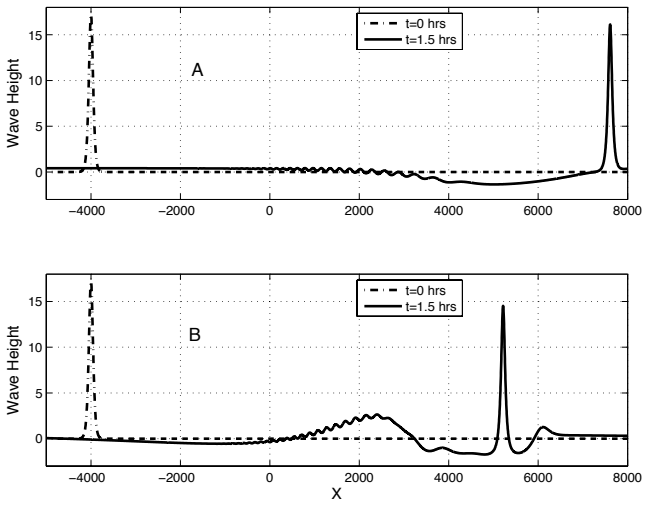

FIGURE 10. The evolution and radiative decay of a KdV solitary wave for the fully dispersive model after 1.5 hours. Panels (A) and (B) show the cases of low ($f = 0.00071$ s^{-1}) and medium ($f = 0.0030$ s^{-1}) rotation, respectively.

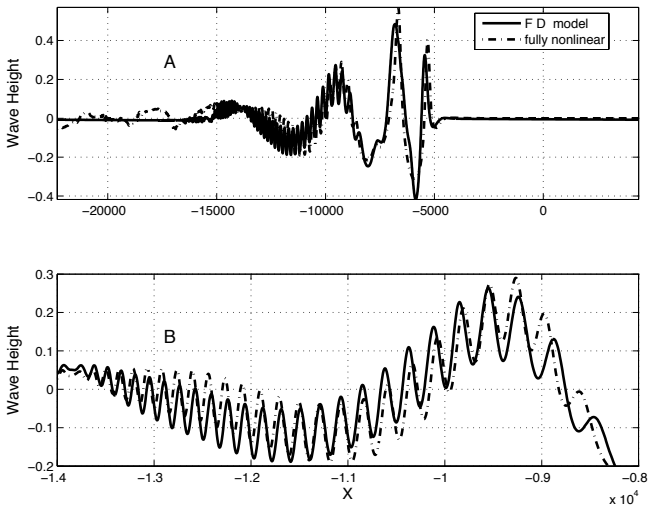

FIGURE 11. The evolution of an initial disturbance (figure 8, panel (A)) taken from a simulation of the full Euler equations. Panel (A) shows the prediction of the fully dispersive model (solid) and the fully nonlinear simulation (dot-dashed). Panel (B) shows the detail of the dispersive wave-tail. $f = 0.0030$ s^{-1} or medium rotation. Both panels are $1,400$ seconds after the initial state.

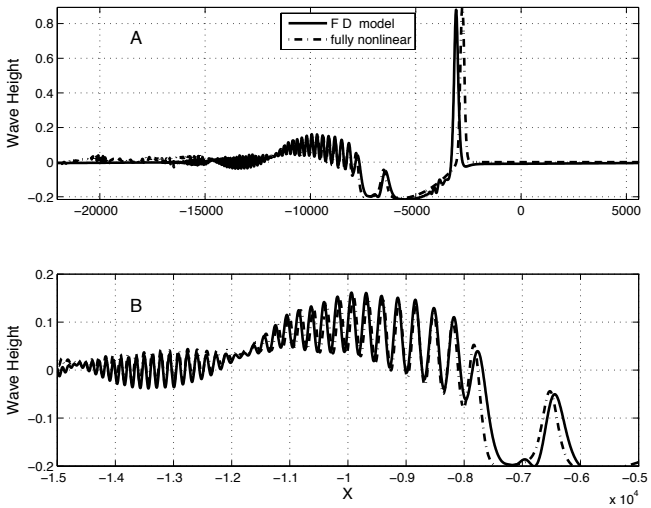

FIGURE 12. The evolution of an initial disturbance (figure 8, panel (A)) taken from a simulation of the full Euler equations. Panel (A) shows the prediction of the fully dispersive (solid) and the fully nonlinear simulation (dot-dashed). Panel (B) shows the detail of the dispersive wave-tail. $f = 0.00071$ s^{-1} or low rotation. Both panels are $1,400$ seconds after the initial state.

Recieved 13 September 2006
E-mail address: mmstastn@uwaterloo.ca; klrowe@student.math.uwaterloo.ca